Cross section measurements of the $^{12}C(n, \alpha_0)^9Be$ and $^{12}C(n, n+3\alpha)$ reactions in the ten-MeV region

Jie Liu[1], Zengqi Cui[1], Yiwei Hu[1], Haofan Bai[1], Cong Xia[1], Zhenpeng Chen[2], Tieshuan Fan[1], Jinxiang Chen[1], Guohui Zhang[1]

Peking University[1]
Tsinghua University[2]
INDEN-LE 20-23 June 2022

Contents

1. Introduction

PEKING UNIVERSITY

- **Carbon**: one of the most widespread elements in nature and organism.
- **(n, lcp) reactions** on carbon in MeV region are of interest for both nuclear technology applications and nuclear physics theories.

Carbon-based neutron spectrometers, e. g. diamond detectors.

Neutron dose calculations in human tissues

Nuclear reaction theories of light elements

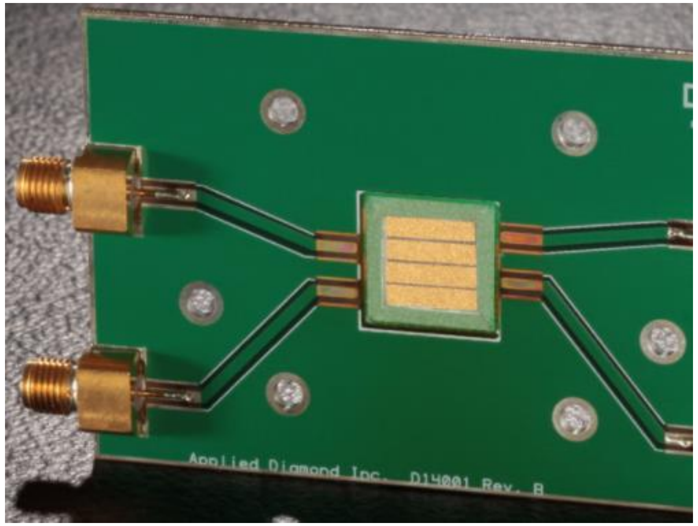

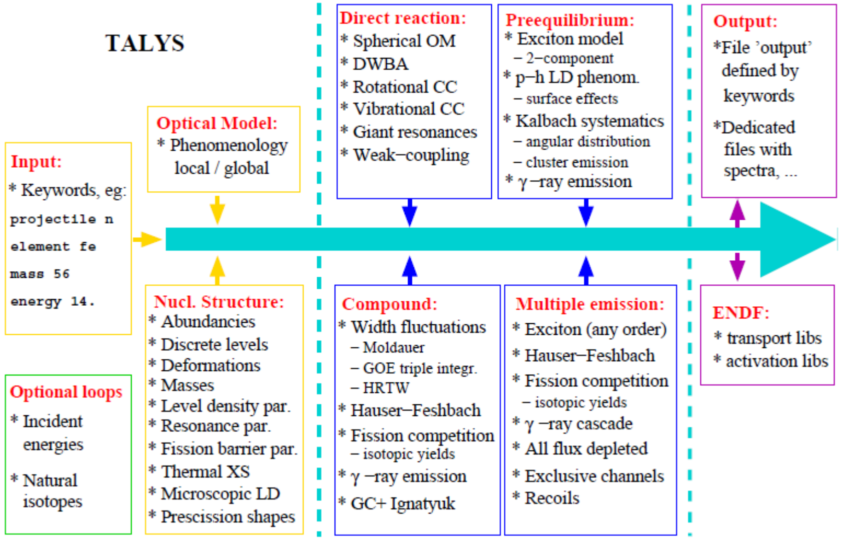

1. Introduction

- **Simultaneous measurements of energy spectrum and fluence of neutrons using a diamond detector;**

  Jie Liu et. al., ***Scientific Reports***, revision submitted.

- **Accurate neutron response matrix**[4-6];

- **Nuclear reaction data.**

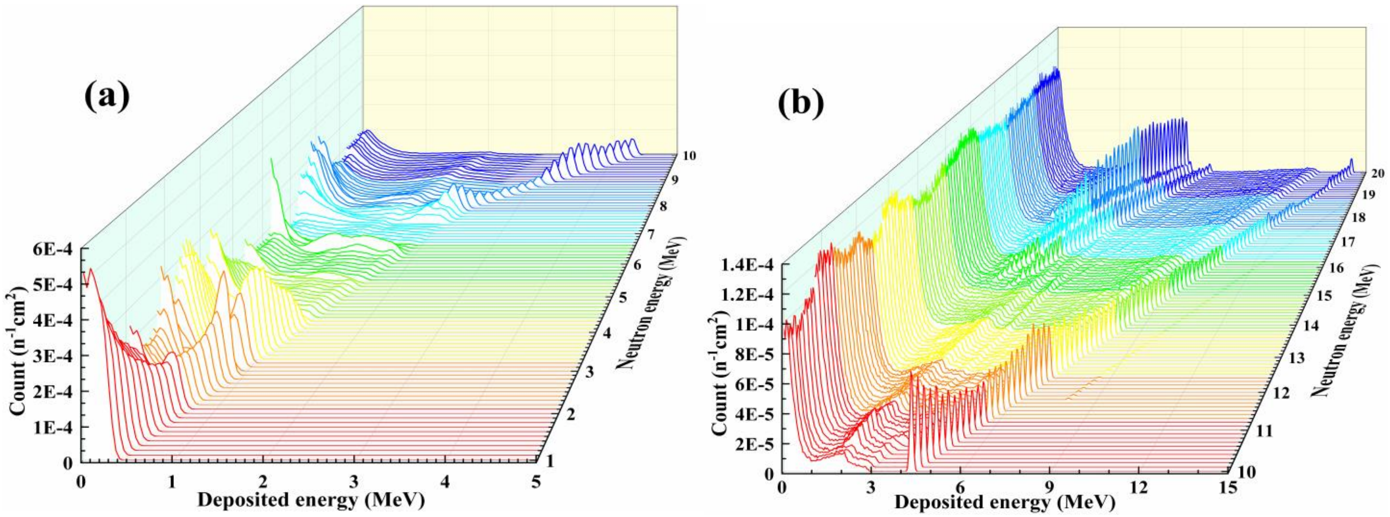

Fig 1. The simulated response matrix of the diamond detector for neutron energies ranging from 1.0 to 10.0 MeV (a) and 10.0 to 20.0 MeV (b).

- **Insufficient accuracy** of the present data for neutron induced reactions on ^{12}C, e. g. ^{12}C(n, n+3α) reaction.

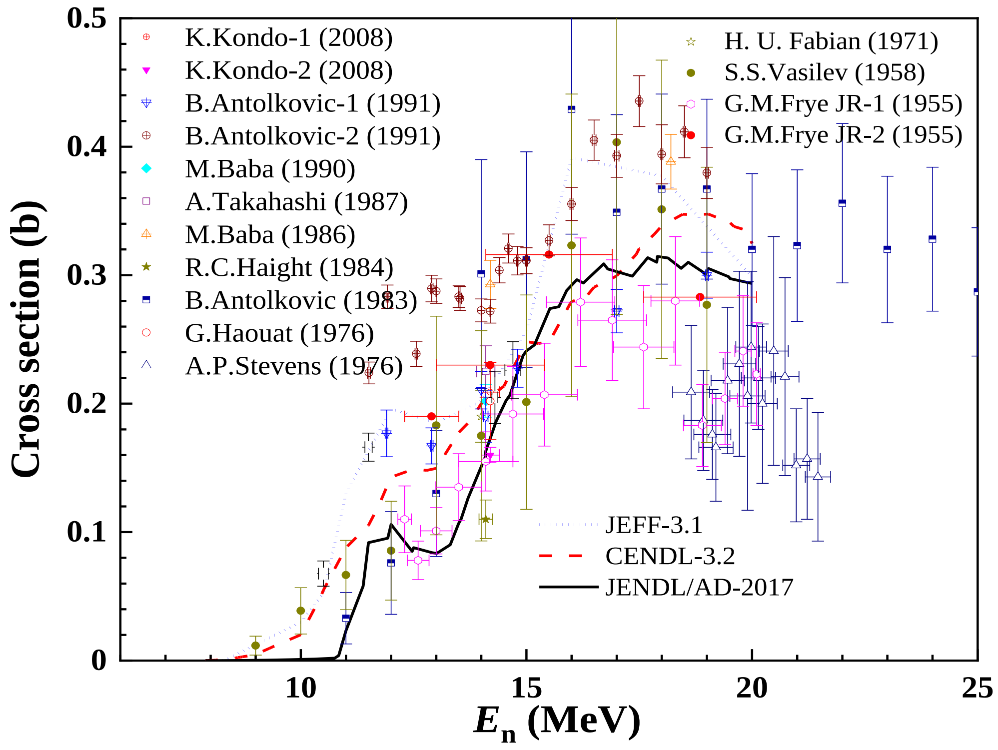

Fig 2. The data of ^{12}C(n, n+3α) reaction

2. Experiments

$^{12}C(n, \alpha_0)^9Be$ & $^{12}C(n, n+3\alpha)$

PEKING UNIVERSITY

Cross section measurements

Neutrons

Samples

Detectors

Neutron fluence measurements

China Institute of Atomic Energy

1. **$^2H(d, n)^3He$** reaction based on **Beijing HI-13 tandem accelerator**, E_n = 9.50, 10.00, 10.50, 11.50 MeV;

2. **$^3H(d, n)^4He$** reaction based on **Cockcroft-Walton generator**, E_n = 14.27 and 14.67 MeV.

Active target

Diamond detector

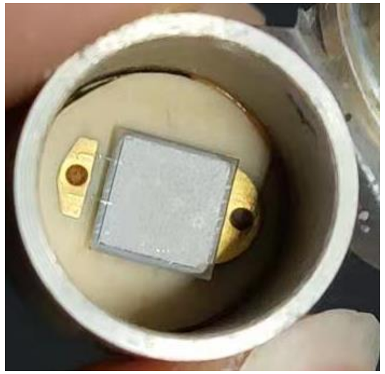

3.8 × 3.8 × 0.50 cm^3

1. **^{238}U (n, f)** reaction;

2. **Associated α particles** from the $^3H(d, n)^4He$ reaction.

2. Experiments

2.1 Experiments based on the HI-13 tandem accelerator

- **Quasi monoenergetic neutrons**: $^{2}H(d, n)^{3}He$ reaction;
- **Neutron fluences**: fission events of the $^{238}U_3O_8$ sample (99.999%);
- **Diamond detector**: active target; at 0-deg with respect to the beam
- **Neutron energy spectra**: EJ-309 liquid scintillator.

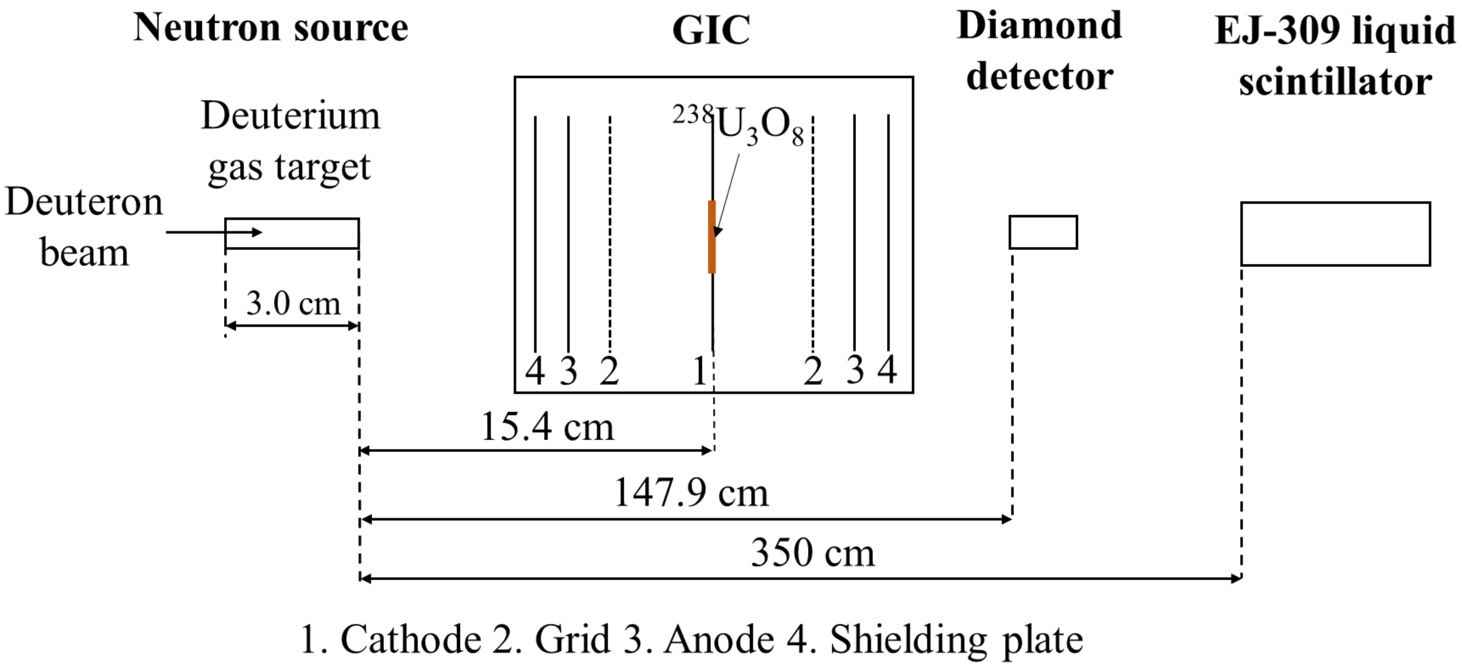

Fig.3 Experimental setup based on the HI-13 tandem accelerator.

2. Experiments

2.2 Experiments based on the Cockcroft-Walton generator

- **Quasi monoenergetic neutrons:** $^{3}H(d, n)^{4}He$ reaction;
- **Au-Si surface barrier detector**: associated α particles from the $^{3}H(d, n)^{4}He$; reaction for measuring the neutron fluences;
- **Diamond detector**: active target.

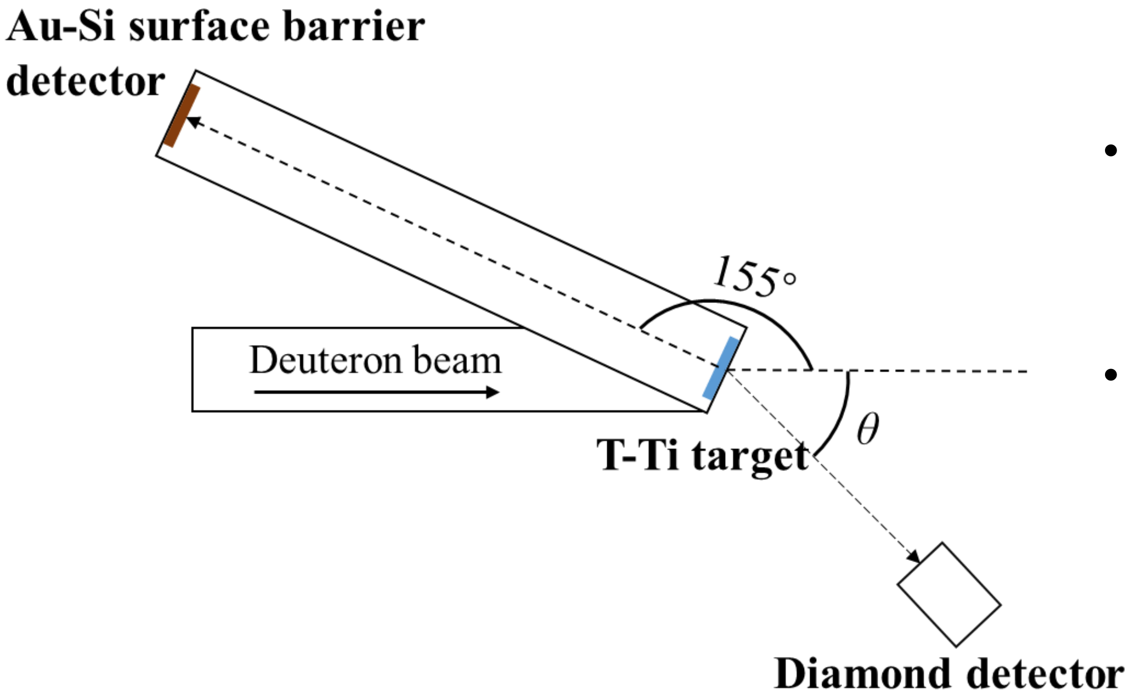

Fig. 4. The experimental setup based on the Cockcroft-Walton generator.

- Positions of the diamond detector: $\theta = 45°$ and $\theta = 80°$.
- E_d = 300 keV, mean neutron energies for the two θ: E_n = 14.27 and 14.67 MeV.

3. Data analysis

北京大學
PEKING UNIVERSITY

Calculation of the cross sections:

$$\sigma = \frac{N_{\text{events}}}{N_{12\text{C}} \cdot \phi}$$

- N_{evens}: Count of the $^{12}C(n, \alpha_0)^9Be$ or $^{12}C(n, n+3\alpha)$ events;
- N_{12C} : Number of the ^{12}C nucleis in the diamond detector;
- ϕ : Neutron fluence at the diamond position.

3. Data analysis

3.1 Determination of the $^{12}C(n, \alpha_0)^9Be$ and $^{12}C(n, n+3\alpha)$ events (N_{evens})

Simulated pulse height spectrum:

- $^{12}C(n, el)$;
- $^{12}C(n, inl)$;
- $^{12}C(n, n+3\alpha)$;
- $^{12}C(n, \alpha_0)^9Be$.

➢ The $^{12}C(n, n+3\alpha)$ events are not determined while E_n is 9.5 and 10.0 MeV: because most of the $^{12}C(n, n+3\alpha)$ events can not be separated from the $^{12}C(n, el)$ events.

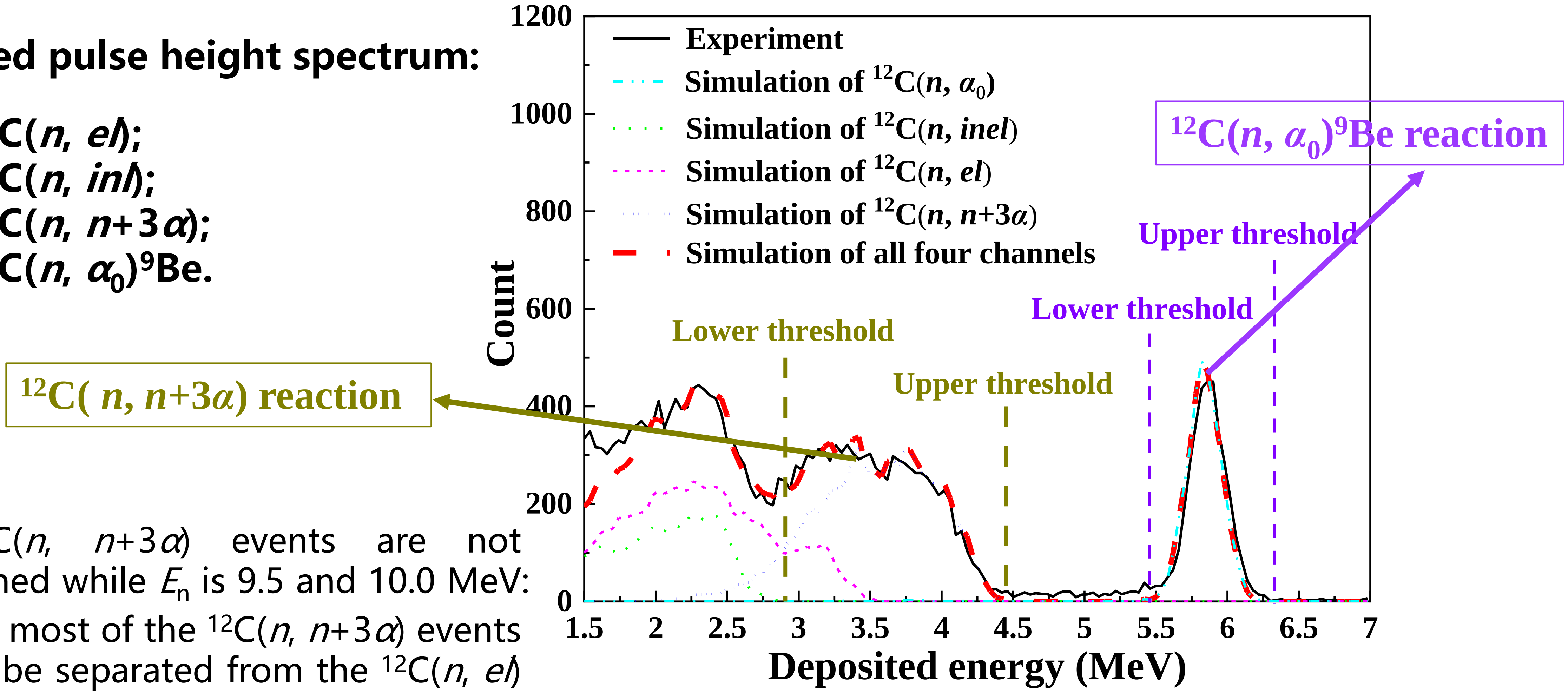

Fig. 5 The measured and simulated pulse height spectrum of the diamond detector at E_n = 11.5 MeV.

3. Data analysis

3.2 Determinations of the neutron fluences (ϕ)

-- for experiments based on the HI-13 tandem accelerator

Fission events of the $^{238}U_3O_8$ sample

$$\phi = \frac{N_f \cdot (1 - K_{low})}{N_{238U} \cdot \varepsilon_f \cdot \sigma_f} R$$

- N_f : count of the fission events between the lower and upper thresholds;
- ε_f : detection efficiency of the fission events;
- N_{238U}: number of the ^{238}U nucleis;
- σ_f : standard cross sections of the ^{238}U(*n*, *f*) reaction[7];
- K_{low}: proportion of the fission events induced by low-energy neutrons;
- *R* : ratio of the neutron fluence at the diamond detector position and that at the $^{238}U_3O_8$ sample position, determined by Monte Carlo simulation.

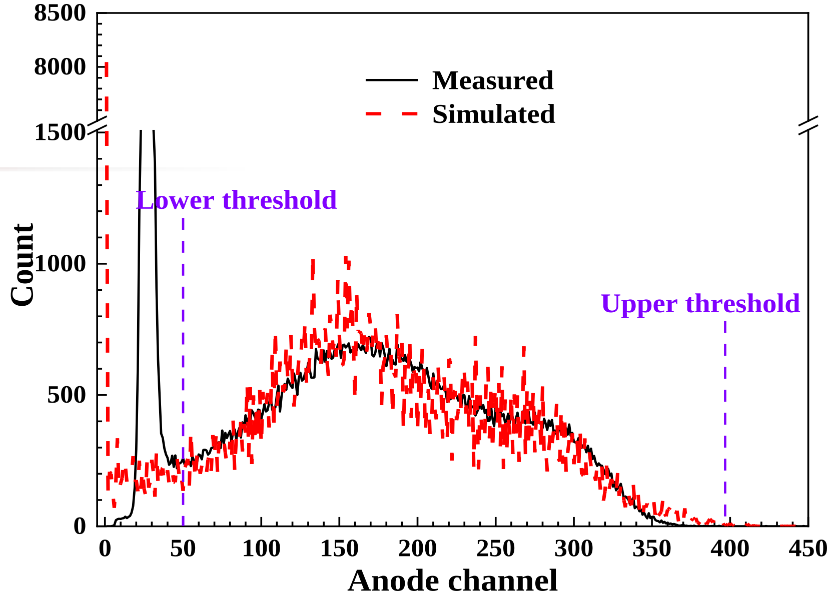

Fig. 6. The anode spectrum of the ^{238}U(*n*, *f*) events at E_n = 11.50 MeV.

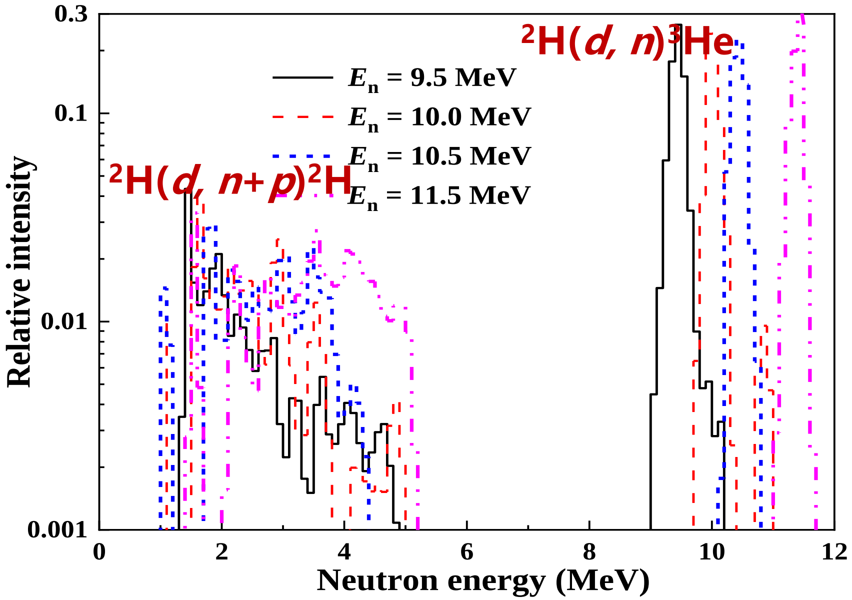

Fig. 7. The neutron energy spectra measured using the EJ-309 liquid scintillator.

3. Data analysis

3.2 Determinations of the neutron fluences (ϕ)

---- for experiments based on the Cockcroft-Walton generator

Alpha particles from the ^{3}H(d, n)^{4}He reaction

$$\phi = \frac{N_{\text{Au-Si}}}{\Omega \cdot d^2} G$$

- $N_{\text{Au-Si}}$: count of the associated alpha particles;
- d : distance between the diamond detector and the T-Ti target;
- Ω : solid angle subtended by the Au-Si surface barrier detector and the T-Ti target;
- G : a factor to correct the different of the angle differential cross sections of the ^{3}H(d, n)^{4}He at the Au-Si surface barrier detector position and the diamond detector position.

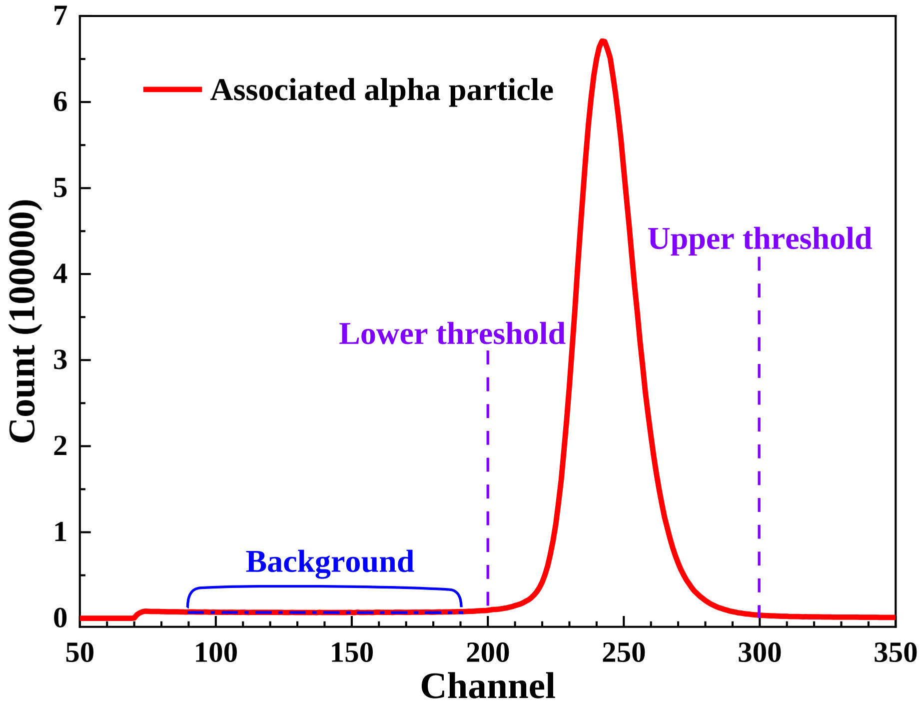

Fig. 8. The energy spectrum of the associated alpha particles measured by the Au-Si surface barrier detector at E_n = 14.27MeV.

4. Results

4.1 Uncertainty analysis

Experiments based on HI-13 tandem accelerator

Source	Uncertainty (%)
N_{evens} for (n, α_0)	**3.7 – 6.6**
N_{evens} for $(n, n+3\alpha)$	**5.4 – 14.1**
N_{12C}	1.0
N_f	0.41 – 0.58
N_{238U}	1.0
ε_f	0.9 – 1.3
σ_f	1.5
K_{low}	1.5 – 2.8
R	1.5 – 3.0

Experiments based on Cockcroft-Walton generator

Source	Uncertainty (%)
N_{evens} for (n, α_0)	**2.9 – 4.4**
N_{evens} for $(n, n+3\alpha)$	**8.2 – 8.3**
N_{12C}	1.0
$N_{Au\text{-}Si}$	0.9 – 1.3
Ω	5.0
G	0.14 – 0.20
d	0.5 – 1.1

- Uncertainties of $^{12}C(n, \alpha_0)^9Be$ cross section: **5.4 - 7.5%**;
- Uncertainties of $^{12}C(n, n+3\alpha)$ cross section : **6.6 - 14.5%.**

4. Results

4.2 $^{12}C(n, \alpha_0)^9Be$ reaction

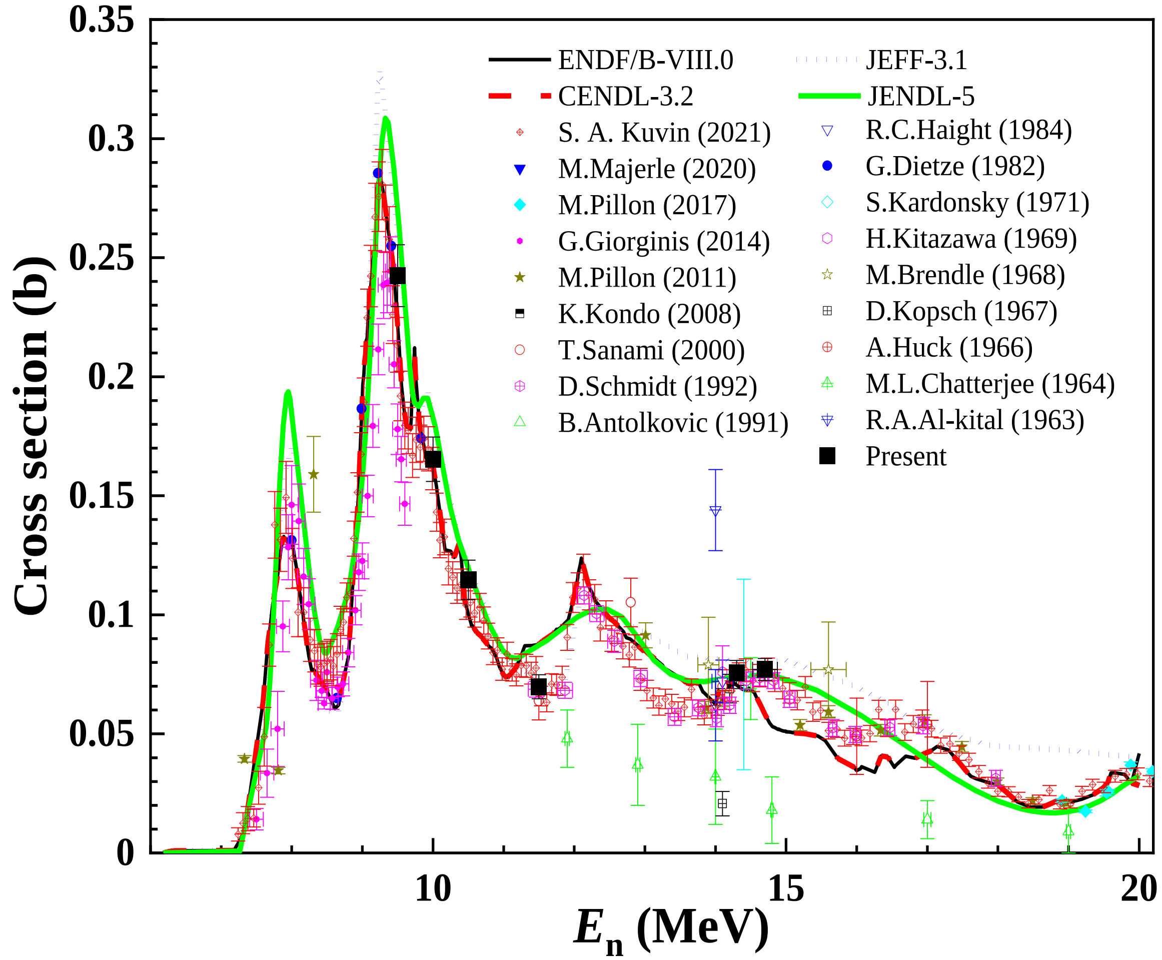

Fig . 9. The cross sections of the $^{12}C(n, \alpha_0)^9Be$ reaction.

- In general, present results are in agreement with the evaluated data from JEFF-3.1[8].
- In the range of 9.0 – 11.0 MeV, present results are in agreement with the evaluated data from ENDF/B-VIII.0[9], JEFF-3.1[8], CENDL-3.2[10] and JENDL-5[11] libraries.
- In the range of 11.0 – 12.5 MeV, present results, the data by Kuvin[12] *et al.* and Schmidt[13] *et al.* are all in agreement with the evaluated data from JEFF-3.1[8].
- The cross sections around 14 MeV vary slowly with the neutron energy, in agreement with the evaluated data from JEFF-3.1[8] and JENDL-5[11] libraries.

4. Results

4.3 $^{12}C(n, n+3\alpha)$ Reaction

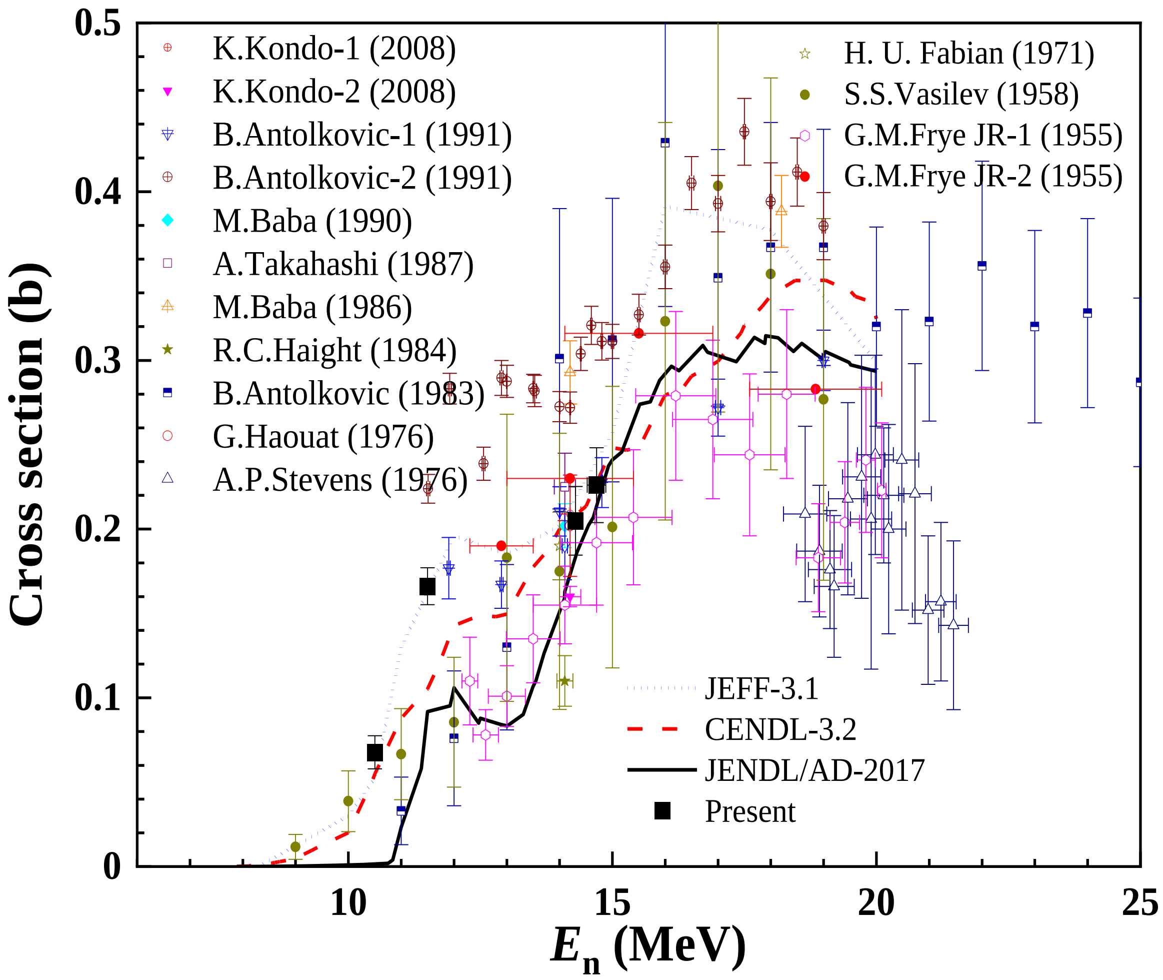

Fig. 10. The cross sections of the $^{12}C(n, n+3\alpha)$ reaction.

- Present results have higher accuracy than previous data.
- In the range of 10.0 – 12.0 MeV, present cross sections are in agreement with the evaluated data from JEFF-3.1[8].
- Around 14 MeV, present cross sections agree with the evaluated data of JEFF-3.1[8], CENDL-3.2[10] and JENDL/AD-2017[14] and the previous measurement results from Kondo-1[15] *et al.* , Antolkovic-1[16] *et al.* and Baba[17] *et al.*

4. Results

4.4 R-matrix analysis - by Prof. ZhenPeng Chen using RAC

- **For n + ^{12}C, the reaction channels:**

(n, tot)=

(n, el)+(n, inl)+(n, a)+(n, p)+(n, d)+(n, t)+(n, g)+

(n，2n)+(n, n+3a)+

(n, x)

- The seven parts in the first row are two-body reaction channels: **specific reaction channels in RAC**;

- The two parts in the second row are multi-body reaction channels: **total width of reduced trace;**

- (n, x) represents the other reaction channels without experimental data.

- The level scheme of ^{13}C from Chen[18] was used as primary values, some levels from Ajzenberg[19] was added in RAC.

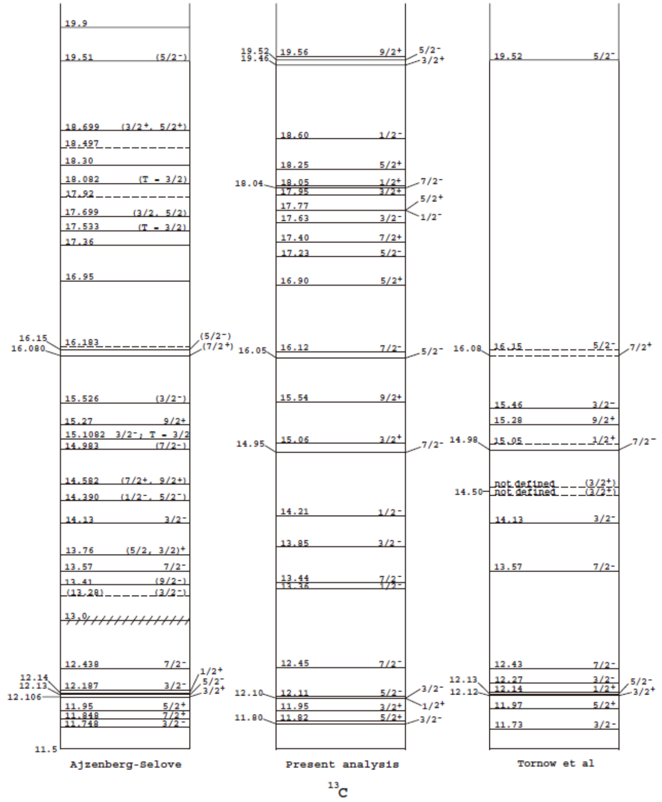

Fig. 11. The level scheme of ^{13}C

4. Results

4.4 R-matrix analysis - by Prof. ZhenPeng Chen using RAC

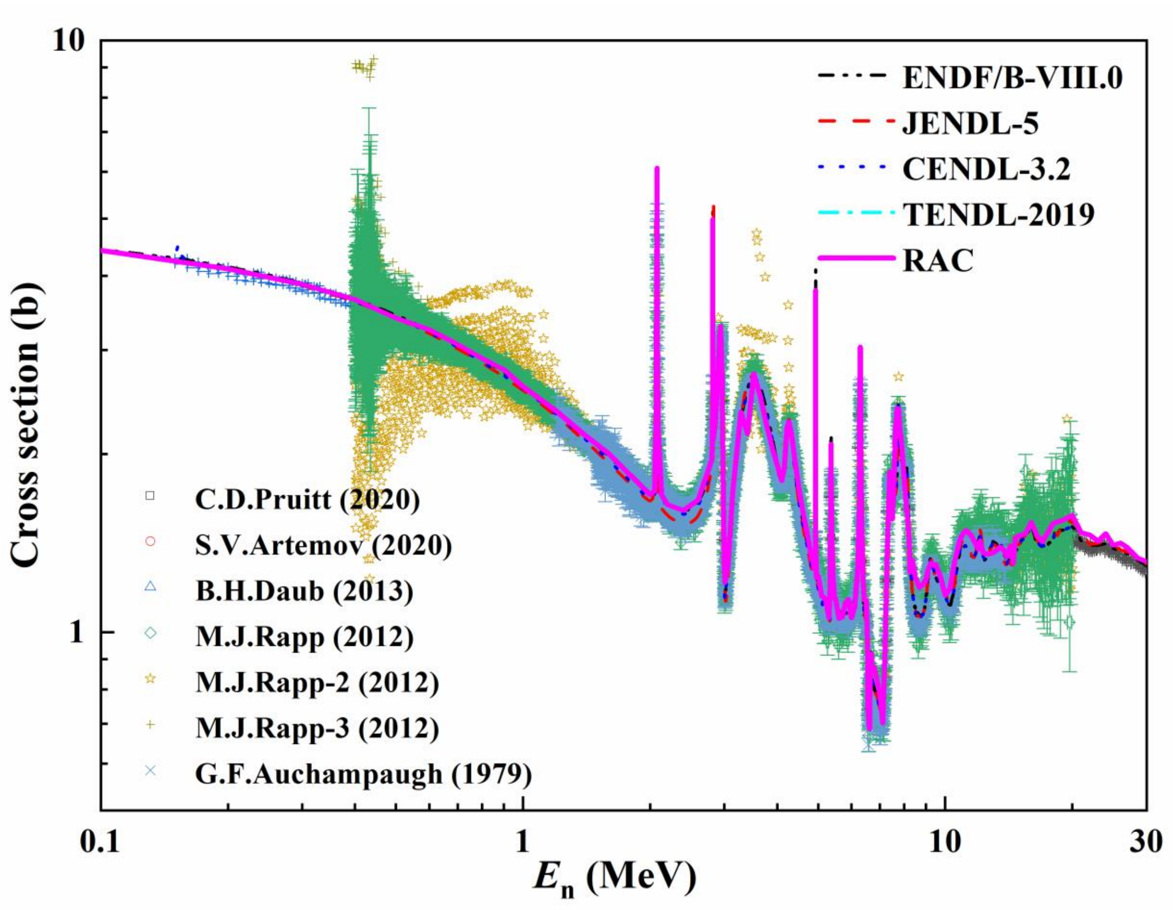

$^{12}C(n, tot)$ reaction

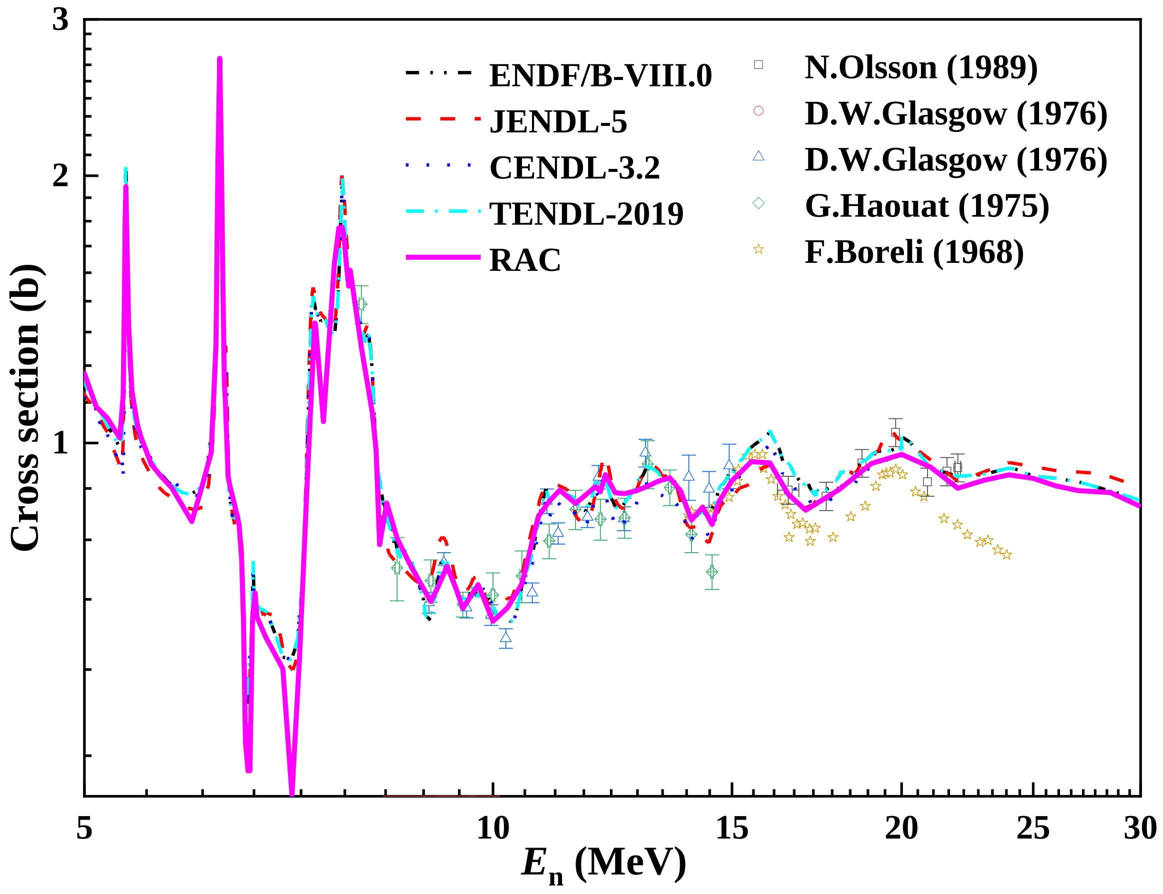

$^{12}C(n, el)$ reaction

4. Results

4.4 R-matrix analysis - by Prof. ZhenPeng Chen using RAC

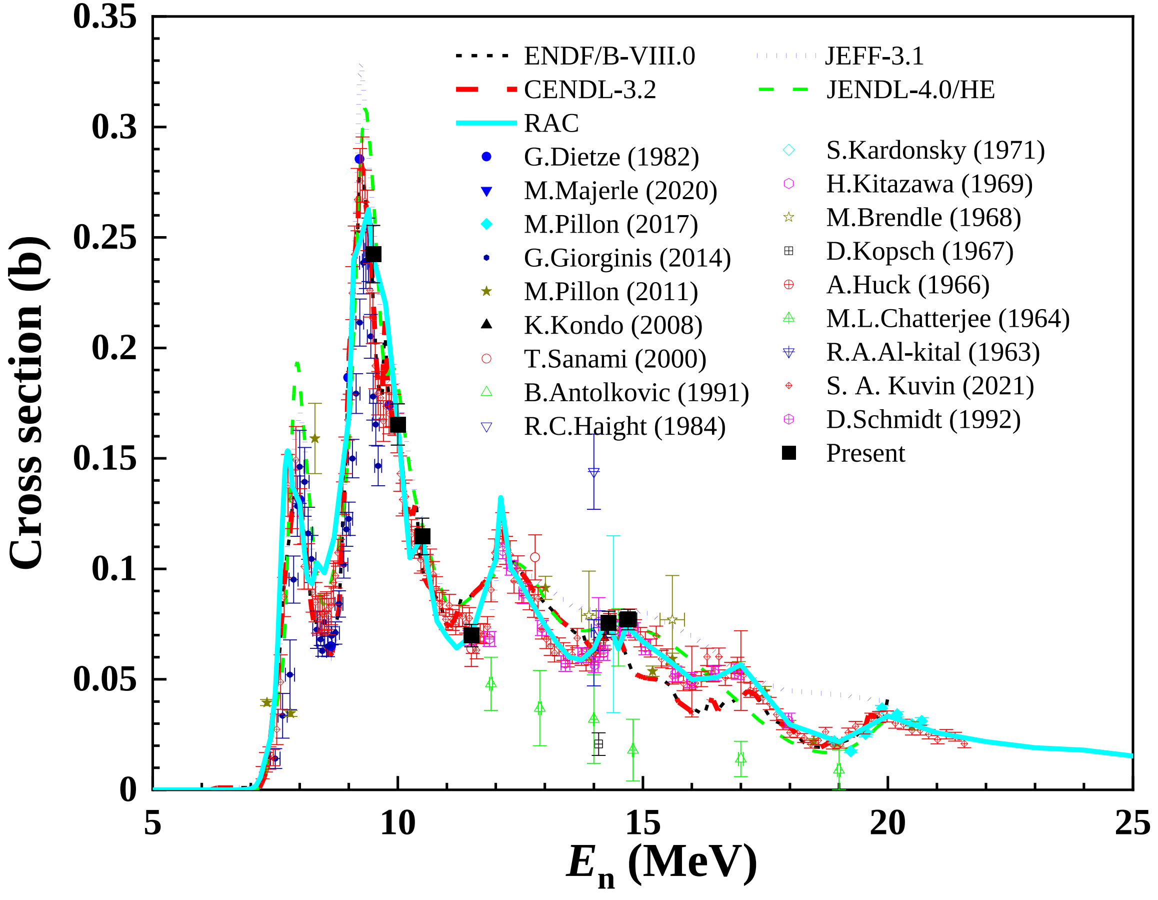

$^{12}C(n, \alpha_0)$ reaction

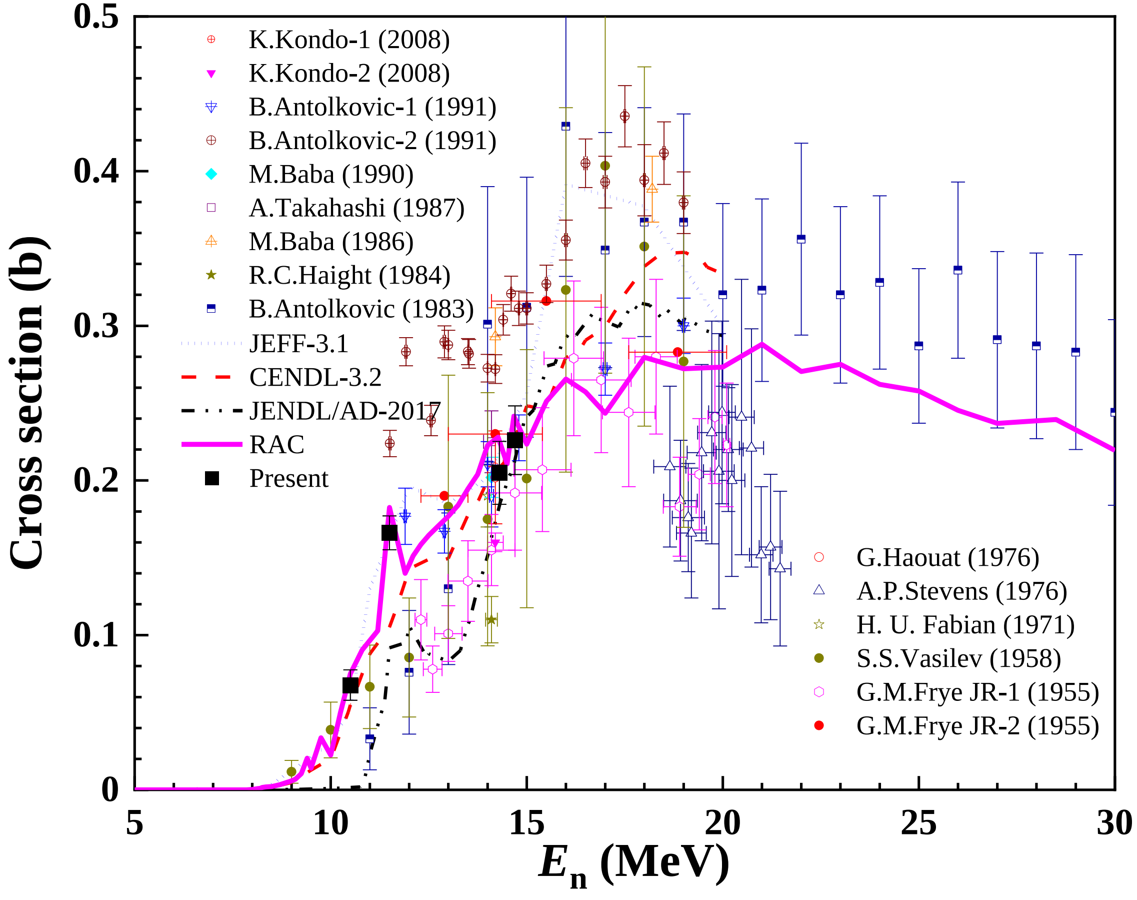

$^{12}C(n, n+3\alpha)$ reaction

4. Results

4.4 R-matrix analysis - by Prof. ZhenPeng Chen using RAC

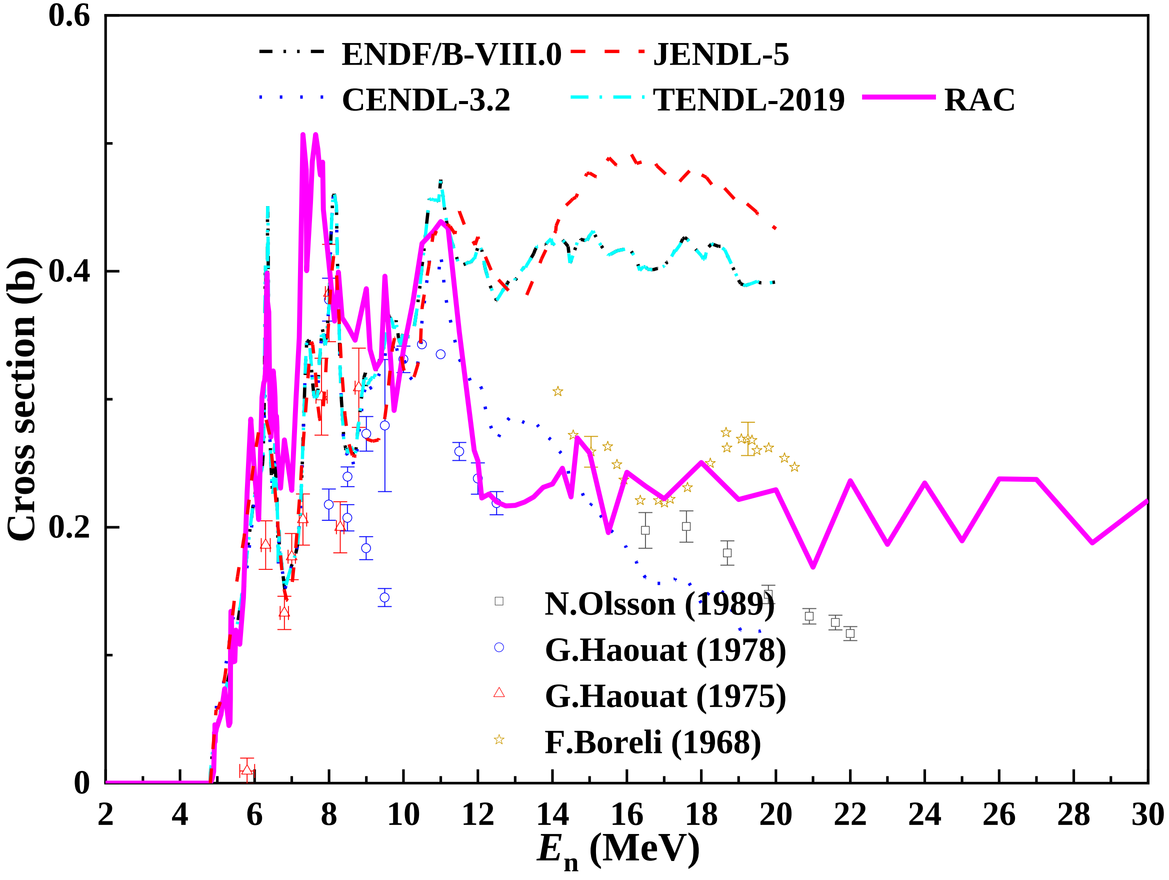

$^{12}C(n, inl)$ reaction

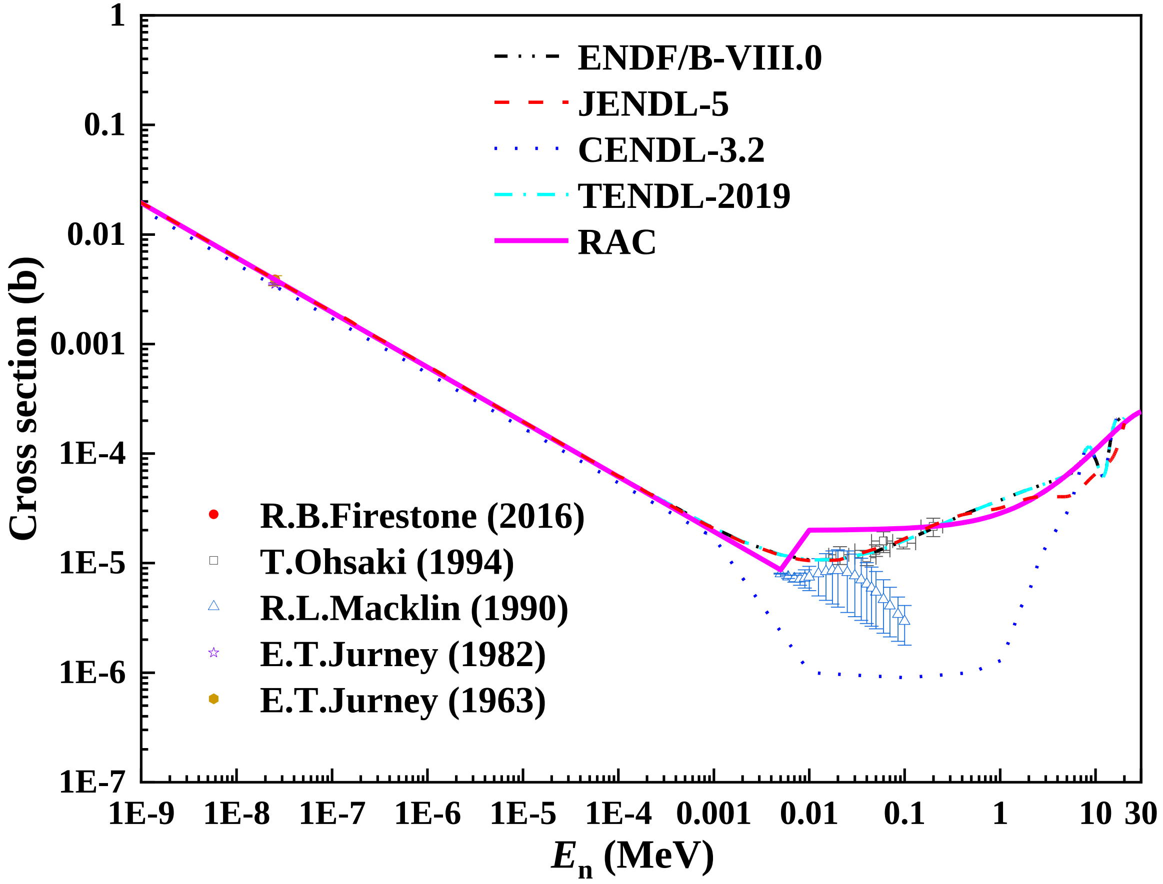

$^{12}C(n, g)$ reaction

4. Results

4.4 R-matrix analysis - by Prof. ZhenPeng Chen using RAC

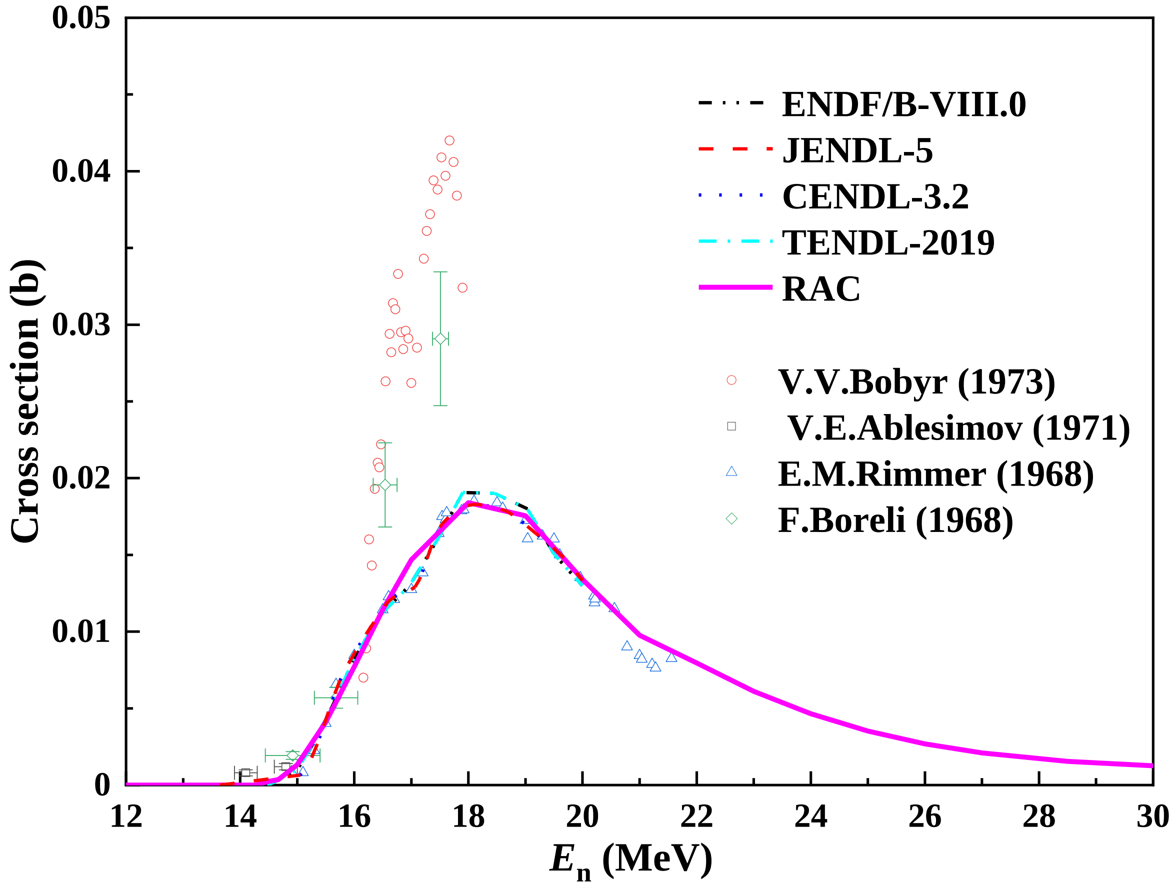

^{12}C(*n*, *p*) reaction

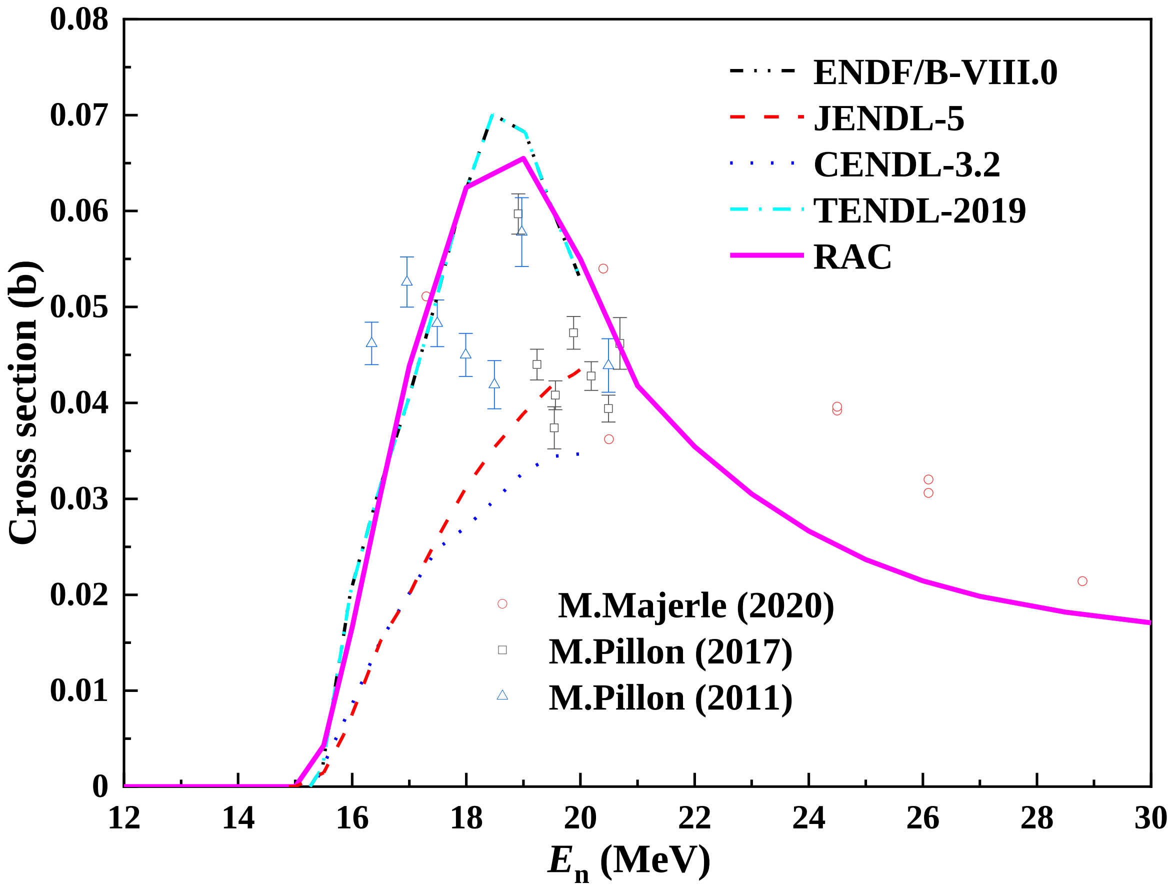

^{12}C(*n*, *d*) reaction

5. Conclusions

北京大學
PEKING UNIVERSITY

- **Cross sections of the $^{12}C(n, \alpha_0)^{9}Be$ and $^{12}C(n, n+3\alpha)$ reactions were measured with higher accuracy in the ten-MeV region using a diamond detector as an active target;**
- **The cross sections of the two reactions were measured simultaneously, which could be checked against each other;**
- **The present results are useful to clarify the deviations among the measurements and evaluations;**
- **R-matrix analysis for the n + ^{12}C system were carried out using the RAC code, and reasonable results were obtained.**

Future works

北京大学
PEKING UNIVERSITY

Paper preparation …

Theoretical analysis of the two reactions …

More neutron energy points …

More reactions, i. e. $^{14}N(n, \alpha)$ and $^{16}O(n, \alpha)$ …

Thank you!

References

[1] M. Marinelli, *et al.*, *Appl. Phys. Lett.* 90, 183509 (2007). https://doi.org/10.1063/1.2734921.
[2] W. Adam, *et al.*, *Nucl. Instrum. Methods Phys. Res., Sect. A* 434, 131 (1999). https://doi.org/10.1016/S0168-9002(99)00447-7.
[3] M. Willander, *et al.*, *Mater. Sci: Mater. Electron.* 17, 1 (2006). https://doi.org/10.1007/s10854-005-5137-4.
[4] L. Giacomelli, *et al.*, *Rev. Sci. Instrum.* 87, 11D822 (2016). https://doi.org/10.1063/1.4960307.
[5] M. Rebai, *et al.*, *Rev. Sci. Instrum.* 87, 11D823 (2016). https://doi.org/10.1063/1.4960490.
[6] M. Rebai, *et al.*, *J. Instrum.* 8, P10007 (2013). https://doi.org/10.1088/1748-0221/8/10/P10007.
[7] A. D. Carlson, *et al.*, Nucl. Data Sheets 148, 143-188 (2018). https://doi.org/10.1016/j.nds.2018.02.002.
[8] JEFF-3.1, https://www.oecd-nea.org/dbdata/nds_jefreports/jefreport-21/jeff21.pdf.
[9] D. A. Brown, *et al.*, Nucl. Data Sheets 148, 1-142 (2018). https://doi.org/10.1016/j.nds.2018.02.001.
[10] CENDL-3.2, http://www.nuclear.csdb.cn/pingjia.html
[11] O. Iwamoto, *et al.*, EPJ Web Conf. 239, 09002 (2020). https://doi.org/10.1051/epjconf/202023909002.
[12] S. A. Kuvin, *et al.*, Phys. Rev. C 104, 014603 (2021). https://doi.org/10.1103/PhysRevC.104.014603.
[13] D. Schmidt, *et al.*, Rept: Phys. Techn. Bundesanst., Neutronenphysik Reports, No. 8 (1992).
[14] K. Shibata, *et al.*, JAEA-Conf 2016-004, pp.47-52.
[15] K. Kondo, *et al.*, J. Nucl. Sci. Technol. 45, 2 (2008). https://doi.org/10.1080/18811248.2008.9711420.
[16] B. Antolkovic, *et al.*, Nucl. Sci. Eng. 107, 1 (1991). https://doi.org/10.13182/NSE91-A23777.
[17] M. Baba, *et al.*, Conf. on Nucl. Data for Sci. and Technol. p.474 (1991).
[18] Z. P. Chen, *et al.*, J. Phys. G: Nucl. Part. Phys. 31 (2005) 1249–1274.http://dx.doi.org/10.1088/0954-3899/31/11/010.
[19] F. Ajzenberg-Selove, Nucl. Phys. A 523 1 (1991).